processes

MDPI

Article

Development of a DNN Predictive Model for the Optimal Operation of an Ambient Air Vaporizer of LNG

Jong-Ho Shin [1], Seung-Kil Lim [2], Jae-Gon Kim [3], Geun-Cheol Lee [4] and June-Young Bang [2,*]

[1] Department of Industrial Engineering, Chosun University, Gwangju 61452, Republic of Korea; jhshin@chosun.ac.kr
[2] Department of Industrial and Management Engineering, Sungkyul University, Anyang-si 14097, Republic of Korea; seungkil@sungkyul.ac.kr
[3] Department of Industrial and Management Engineering, Incheon National University, Incheon 22012, Republic of Korea; jaegkim@inu.ac.kr
[4] College of Business Administration, Konkuk University, Seoul 05029, Republic of Korea; gclee@konkuk.ac.kr
* Correspondence: jybang@sungkyul.ac.kr

Abstract: In this study, we conducted preliminary research with the objective of leveraging artificial intelligence to optimize the efficiency and safety of the entire Ambient Air Vaporizer (AAV) system for LNG (Liquid Natural Gas). By analyzing a year-long dataset of real operational data, we identified key variables that significantly influence the outlet temperature of Natural Gas (NG). Based on these insights, a Deep Neural Network (DNN) prediction model was developed to forecast the NG outlet temperature. The endeavor to create an effective prediction model faced specific challenges, primarily due to the narrow operational range of fan speeds and safety-focused guidelines. To surmount these obstacles, various learning algorithms were evaluated under multiple conditions. Ultimately, a DNN model exhibiting lower values of both absolute mean error (MAE) and mean square error (MSE) was successfully established.

Keywords: LNG; ambient air vaporizer; DNN; prediction model; real factory data analysis

check for updates

Citation: Shin, J.-H.; Lim, S.-K.; Kim, J.-G.; Lee, G.-C.; Bang, J.-Y. Development of a DNN Predictive Model for the Optimal Operation of an Ambient Air Vaporizer of LNG. *Processes* **2023**, *11*, 3143. https://doi.org/10.3390/pr11113143

Academic Editor: Jiaqiang E

Received: 17 October 2023
Revised: 31 October 2023
Accepted: 1 November 2023
Published: 3 November 2023

1. Introduction

In recent years, the 4th industrial revolution has gained momentum in the manufacturing industry, driven by the innovative use of big data. Within the manufacturing sector, the main application of big data has traditionally been concentrated on image-based detection of defects in semi-finished and finished products, as well as quality-control-related activities. However, recent research has revealed an expanded array of big data applications within this field. By incorporating big data technology into manufacturing processes, significant advancements in accuracy and precision have been realized across various aspects such as planning, production, and logistics. This integration is not only leading to enhanced efficiency but also fueling a growing demand for the utilization of big data to augment equipment safety and performance.

Building upon this emerging paradigm, this paper presents a novel model designed to predict the NG (Natural Gas) discharge temperature of the pneumatic vaporizer in a liquefied gas vaporization facility, employing field data. The proposed methodology harnesses artificial intelligence models, positioning itself as an essential tool for maximizing the operational efficiency of pneumatic vaporizers. Furthermore, the implications of this model extend beyond mere efficiency enhancements. It also offers valuable support for operation automation, meticulously considering vital safety parameters. This advancement symbolizes a broader shift towards data-driven solutions in the manufacturing sector that synergize efficiency, innovation, and safety. Ultimately, this research underscores the transformative role of big data, heralding a new era of possibilities in manufacturing technology and methodologies.

When transporting natural gas from one continent to another, the volume of the gas is reduced through liquefaction, converting it from a gaseous state to a liquid state for more efficient shipping by sea. Once delivered, the liquefied natural gas (LNG) is stored in tanks at a vaporization facility, where it is gasified in accordance with demand by using vaporizers. It is then distributed through natural gas (NG) supply pipes to various demand sites. NG is not only supplied to households via urban gas pipelines but also serves as fuel for natural-gas-powered power plants and large industrial complexes (Figure 1).

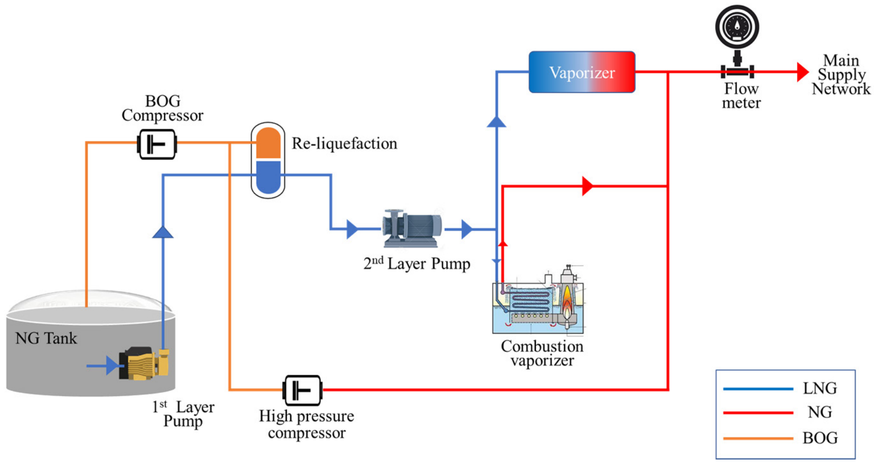

Figure 1. LNG to NG Production Process.

The vaporization of liquefied natural gas (LNG) to natural gas (NG) is the crucial process within a liquefied gas vaporization facility, and the vaporizer plays a pivotal role in the NG production process. Various types of vaporizers are utilized, including: (1) the open rack vaporizer (ORV), which employs seawater as a heat source via heat exchange, and (2) the ambient air vaporizer (AAV), which utilizes ambient air as a heat source. The ORV (Figure 2) is generally more efficient in vaporizing NG than the AAV due to the higher heat capacity of seawater compared to ambient air. However, the ORV can negatively impact the marine ecosystem by reducing the seawater temperature near the plant. Conversely, the AAV (Figure 3) minimizes its impact on the surrounding ecosystem by quickly discharging and dispersing the warmed air during the vaporization of LNG. Within the AAV system, LNG is injected into the heat exchanger's inlet, and fans atop the vaporizer tower circulate the ambient air. This air flows briskly from the top to the bottom of the heat exchanger and then scatters into the surrounding atmosphere, reducing environmental impact.

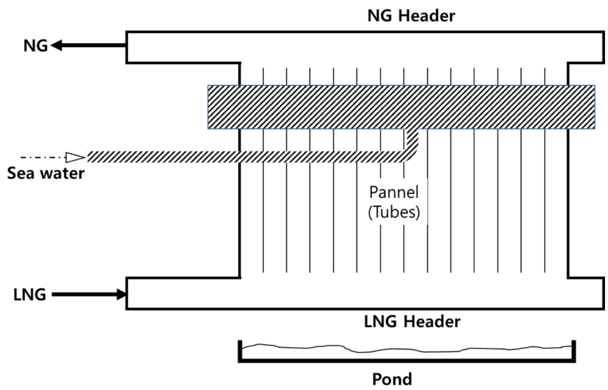

Figure 2. Open rack vaporizer.

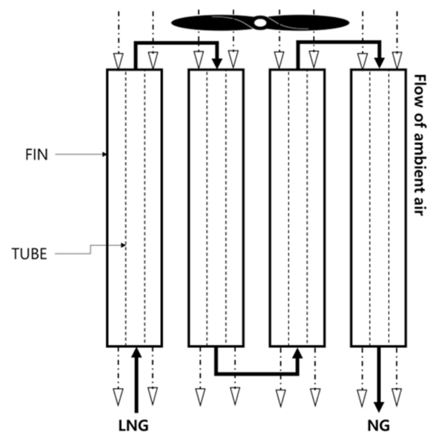

Figure 3. Inside of an open rack vaporizer's cell. As NG flows through the tube, it vaporized. Concurrently, a fan is activated to expel the resultant chilled air.

As described above, the Ambient Air Vaporizer (AAV) is a more environmentally friendly option, with reduced impact on the surrounding environment. However, it does have some limitations, particularly in terms of efficiency. The heat capacity of ambient air is less than that of water, leading to lower heat exchange efficiency, especially when the "icing phenomenon" occurs. This phenomenon happens when ice forms on the fins during the heat exchange process, hindering the efficiency. To resolve this issue, a defrosting operation must be carried out periodically. During this operation, the fan at the top of the vaporizer works without LNG flow to remove the ice around the heat exchanger's fins. In favorable weather conditions with high temperatures and low humidity, the vaporization process can be maintained for longer periods. Conversely, in conditions of low temperatures and high humidity, the icing phenomenon is more likely, and the fans must circulate more quickly to sustain the vaporization. Therefore, the efficient operation of the AAV depends on carefully controlling the fan's rotational speed (RPM) in line with atmospheric conditions to keep the vaporization process running as long as possible.

In the present investigation, a Deep Neural Network (DNN)-based prediction model has been meticulously devised to predict the outlet NG temperature of the Ambient Air Vaporizer (AAV), contingent on input variables such as the fan's Rotations Per Minute (RPM) atop the heat exchanger within the AAV, in conjunction with the inlet temperature and flow rate of LNG. The rest of this manuscript is organized as follows. Section 2 surveys antecedent works pertinent to the utilization of artificial intelligence in both operation and natural gas (NG) production plants. Section 3 describes the architecture of the AAV and delineates its operational procedures, while concomitantly defining the problem under investigation in detail. Section 4 provides a comprehensive account of the preprocessing and analysis procedures of extant real operation data of AAV, and isolates significant input data germane to the outlet temperature of NG from the scrutiny of this data. Also, Section 4 elucidates the predictive DNN modeland validates the model's accuracy through empirical analysis of field data. Finally, Section 5 succinctly encapsulates the contributions of the present study and proffers directions for prospective research endeavors.

In the engineering plant industry, large and intricate machinery operate systematically to produce products by consuming energy or vital resources. Like many other industrial sectors, engineering plants have been making great efforts over the past several years to achieve production optimization by applying machine learning to their operational controls. In particular, research in the specialized field of predictive control has emerged as one of the most promising approaches toward this end. The progress and realization of this objective have been the subject of several scholarly investigations. Zhang et al. (2017) suggested a generalized architecture that utilizes big data analytics to improve Product Lifecycle Management (PLM) and to enhance decision-making processes for production [1]. Reddy et al. (2019) developed data-driven empirical models specific to LNG BOG (boil-off gas) compressors, demonstrating superior performance over traditional Artificial Neural Network (ANN) and Kriging models [2]. Walther et al. (2019) engaged traditional machine learning algorithms such as Random Forest (RF), Extremely Randomized Trees, and Gradient Boosting Regression Trees with the objective of forecasting the short-term electric load within a factory setting [3]. Park et al. (2020) conducted an exploration to identify critical factors influencing the quality of steel plate manufacturing, subsequently utilizing machine learning to predict these variables [4]. Complementing these studies, Mohamadi and Ehteram (2020) engineered a machine learning model capable of predicting the monthly evaporation of water resources with marked accuracy [5].

Another significant domain of application for machine learning within plant engineering pertains to decision-making processes and defect detection in products, aimed at facilitating preventive maintenance of facilities. A comprehensive synthesis of cases and research findings, wherein machine learning algorithms have been employed for preventive maintenance, has been meticulously catalogued in the survey paper by Carvalho et al. (2019) [6]. The task of defect detection in products has been the subject of rigorous investigation, traditionally employing methods geared toward classifying product images. In more recent developments, Convolutional Neural Network (CNN)-based models have emerged as the principal approach for determining product defects. Westphal and Seitz (2021) advanced this field by proposing a sophisticated transfer learning (TL) method, leveraging both the VGG16 and Xception CNN models explicitly for defect detection [7]. Their study utilized non-destructive test data, with the VGG16-model-based TL method demonstrating a markedly high level of accuracy in comparison to alternative models. Complementing this, Zhang et al. (2021) explored various classifiers, including Long Short-Term Memory (LSTM) and Backpropagation Neural Network (BPNN), specifically for acoustic test data, in order to discern defects in glass bottles, subsequently evaluating the accuracy of these models [8].

This study delves into the application of machine learning algorithms specifically for optimization within the domain of LNG or NG production operations. Related research in this field includes the following contributions. Adib et al. (2015) constructed an SVM-based predictive model to gauge hydrogen sulfide pressure during the removal process, utilizing input data such as top stabilizer column pressure, temperature, seal pressure, and volumetric flow rate of the condition [9]. Zhou et al. (2020) employed diverse machine learning models, including ANN, Random Forest, AdaBoost, and XGBoost (Extreme Gradient Boosting), to anticipate the heat transfer coefficient of a capacitor, a component possessing a function contrary to that of a vaporizer [10]. The research findings revealed that these algorithms could robustly predict condition heat transfer coefficients within mini/microchannels. Complementing these efforts, Wood (2021) designed ANN and transparent open-box learning network (TOB) models to refine tank pressure control, subsequently demonstrating that the TOB model yielded more accurate predictions of saturated vapor pressure within tanks than conventional ANN models [11].

Research focusing on the performance of LNG vaporizers can be classified into the realm of traditional heat transfer studies, and our investigation primarily centers on this area. A substantial body of work employing the conventional approach to heat transfer within vaporizers has been conducted, both broadly and in-depth [12–16]. Such studies have emphasized the analysis of vaporization characteristics, utilizing numerical models founded on the underlying equations of heat transfer, and integrating these findings into the optimal design of the vaporizer. In addition to this, there have been recent endeavors to predict vaporizer performance through machine learning, leveraging extensive field data. Notably, Shin et al. (2021) introduced a dynamic prediction model for determining NG outlet temperature and discharge seawater temperature in response to variations in an ORV's seawater flow rate, seawater temperature, and LNG flow rate [17]. The ensuing results indicated that the predictive accuracy as measured in MES followed the sequence of LSTM, AutoML, and FNN. Recently, Chen et. al. (2023) proposed a new hybrid model for predicting the remaining useful life (RUL) of lithium-ion batteries, combining a channel attention (CA) mechanism with long short-term memory networks (LSTM). The model demonstrates strong predictive performance, improving the use of local features in limited data scenarios and mitigating the effects of battery capacity rebound, and its effectiveness is validated using NASA and University of Maryland datasets [18].

Despite substantial efforts to optimize the operation of vaporizers, the application of machine learning technology in this domain remains underexplored. As industries increasingly recognize the need to integrate artificial intelligence within their operational frameworks, the drive to harness its capabilities extends to both the management of production processes and the detection of defects. The primary objective of this paper is to explore the application of artificial intelligence, specifically in enhancing the efficiency of the production process, as well as in the vital task of identifying defects.

2. Problem Description

Liquefied Natural Gas (LNG) flows within the tubes of the heat exchanger, absorbing heat from the warm ambient air outside the tubes, and subsequently being converted into Natural Gas (NG). To facilitate this heat exchange process between the ambient air and LNG, a fan situated above the tubes is activated, thereby increasing the circulation of ambient air. This air is drawn into the upper side of the Ambient Air Vaporizer (AAV) by the fan, channeled through the tubes, and finally discharged at the bottom of the AAV. Since the cooled, discharged air has minimal impact on the surrounding environment, this method is often considered more eco-friendly. However, its efficiency is generally lower than that of combustion or seawater-based systems.

The effective operation of an AAV is more complex than that of other vaporizer types, as the vaporization performance can fluctuate significantly depending on unpredictable atmospheric conditions, such as temperature and humidity. A notable challenge arises when icing forms on the fins of the heat exchanger during the vaporization process, severely hindering heat exchange and causing a drastic drop in efficiency. In some instances, this icing can lead to NG temperatures falling below 0 °C, necessitating a halt in the vaporization process to perform defrosting.

The operational conditions further dictate that when the atmospheric temperature is high and humidity is low, vaporization can persist for an extended period without requiring an increase in fan rotational speed. Conversely, when the temperature and humidity levels are insufficient to maintain the planned vaporization period, the fan's rotational speed must be increased to enhance heat exchange, thus preserving the desired vaporization duration. However, this increased speed leads to greater energy consumption. Therefore, for an energy-efficient operation of the AAV, dynamic control of the fan's rotational speed is imperative, requiring careful adjustment in response to atmospheric conditions during the vaporization period.

Figure 4 illustrates the configuration of Ambient Air Vaporizer (AAV) groups employed in the Natural Gas (NG) production process studied in this research. This particular plant is currently under the management of an NG supply company in South Korea. The vaporization infrastructure encompasses 16 AAV cells, systematically organized into hierarchical groupings. Specifically, two cells are combined to constitute one unit, and two such units are further assembled to create four distinct groups. Within this structure, the two cells that comprise the same unit are synchronized to undertake either the vaporization or defrosting operation simultaneously. Furthermore, within the same group, the two units are coordinated so that they do not operate concurrently; in other words, if one unit is engaged in vaporizing or defrosting, the other remains inactive. This operational design is predicated on the understanding that the simultaneous activation of two adjacent units within the same group can result in a diminished heat exchange performance.

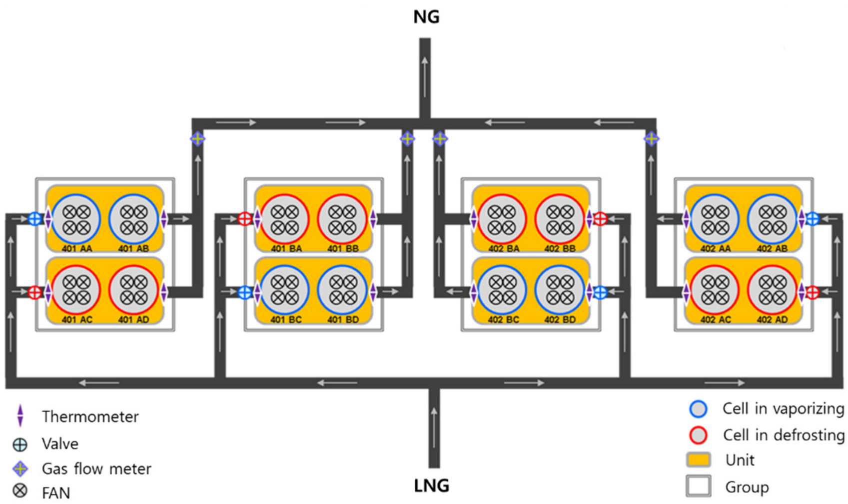

Figure 4. Structure of AAV groups.

However, the system is designed to allow for flexibility, and the two units within a group may operate in tandem if the situation warrants. In such cases, while one unit undertakes the defrosting operation, the other can continue with the vaporization process. This careful orchestration ensures both efficiency and responsiveness to the variable demands of the NG production process.

The production volume of Natural Gas (NG) must align with the demands of gas consumers, thereby dictating the quantity of Liquefied Natural Gas (LNG) dispensed into Ambient Air Vaporizer (AAV) facilities according to NG requirements. In order to manage the flow of LNG through the AAV system, a seasoned operator assesses the number of units required for activation and carefully calibrates the fan speed within these units to match the processing needs. As depicted in Figure 4, an array of data is systematically gathered during the vaporization process to inform operational decisions. Several key parameters are monitored across different stages:

(1) Valve Opening Angle: at the entrance of each AAV unit, the angle of the valve is tracked in degrees to regulate the flow rate of LNG entering the unit;
(2) Temperature Monitoring: the temperatures of both the LNG and NG are observed through thermometers positioned at the inlet and outlet of the tubes within each unit;
(3) Production Quantity: the volume of NG produced by each group is documented using a specialized vaporization flow meter;
(4) Operating States: within individual units, the duration of three distinct operating states—vaporizing, defrosting, and readiness for operation—is recorded;
(5) Vaporizing Period Data: for units in the vaporizing phase, pertinent data such as the rotational fan speed and the time elapsed since the initiation of vaporization are collected;
(6) Ambient Conditions: the surrounding air temperature and humidity levels are monitored, as they can significantly impact the efficiency of the vaporization process.

These multifaceted data points are integral to the precise and efficient control of the AAV system, ensuring that the production of NG is responsive to fluctuating consumer demands.

The aforementioned data collected during the vaporization process constitute time-series information, where the temperature of the produced Natural Gas (NG) at a given moment is closely correlated with these measurements. Throughout the vaporization period, ambient air is drawn from the top of the heat exchanger and expelled at a reduced temperature from the bottom. As this bypassing of ambient air facilitates heat exchange, icing occurs on the surface of the tubes' fins, causing a gradual decrease in the temperature of the produced NG. If the temperature of the produced NG falls below 0 °C, it must be reheated, incurring additional costs. Increasing the rotational fan speed can postpone the point at which the temperature of the produced NG drops below 0 °C. However, the operational cost of the fan, driven by electrical energy, rises in direct proportion to the rotational speed. Therefore, the challenge lies in developing an efficient operational methodology that minimizes energy expenses while maintaining vaporization performance for the targeted duration. Striking this balance requires a nuanced understanding of the interplay between temperature control, fan speed regulation, and energy consumption, highlighting the importance of sophisticated monitoring and control mechanisms within the LNG vaporization process.

At present, the control of the AAV's fan speed and the decision to halt the vaporization operation rely heavily on human expertise, informed by various data collected during the vaporization process. Determining the optimal operation policy based on real-time data fluctuations presents a significant challenge. Predicting the precise moment when the temperature of the produced NG will fall below 0 °C under specific operational policies in a variable environment further complicates this task. To address this complex issue, we introduce a predictive model utilizing a deep neural network. The model aims to forecast the temperatures of produced NG at the outlet of the heat exchanger's tubes—a critical factor in devising an optimal operation policy for the vaporization system. This approach seeks to integrate advanced machine learning techniques with traditional control methods, enhancing accuracy, and efficiency in a continually evolving industrial landscape.

3. Data Preprocessing and Analysis

A fundamental step in developing an artificial intelligence model for predicting NG temperature at the outlet of the heat exchanger involves collecting and preprocessing sensor data, and then transforming these data into suitable features for AI modeling. In this study, raw sensor data were obtained directly from the NG production plant. Since this raw data comes in a format and structure that is not immediately suitable for model development, preprocessing is an essential stage. This section delves into the data preprocessing procedures applied to the sensor data and subsequently presents the results of data analysis on the preprocessed information. The analysis provides valuable insights that guide the design of the AI model's input and output features.

3.1. Data Preprocessing and Refinement

Figure 5 outlines the comprehensive procedure for data preprocessing. Eleven months of raw AAV data, supplied by the NG production plant, encompass various types of information such as cell ID, fan speed, vaporization flow rate, LNG inlet temperature, air temperature, and humidity. Because the time intervals for these collected pieces of information differ, an initial step of time synchronization is performed to address this issue. After this synchronization, all information is converted into a unified time-series format with 10 min intervals to optimize the dataset size. Utilizing the synchronized data, specific information is then prepared for AI training, simulation, and data analysis.

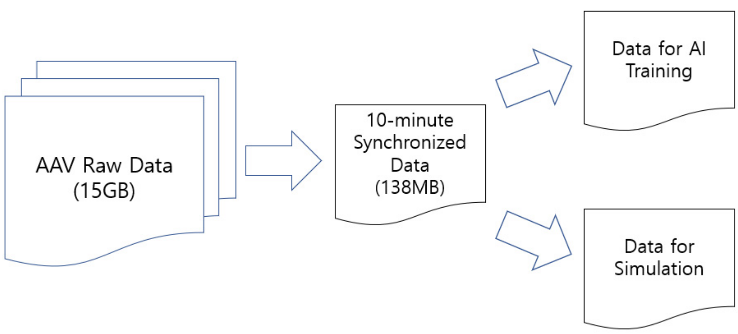

Figure 5. Data Preprocessing Procedure.

In this phase, R—a widely recognized statistical programming language—serves as the software tool for data preprocessing. Given the presence of various time-series data with different collection time points, an initial task involves determining an appropriate time interval to both condense the raw data and synchronize it over a longer duration. For the purpose of this study, a 10 min time interval has been selected. This interval is sufficiently brief to capture the raw data's intricate features, yet wide enough to make the size of the synchronized dataset manageable. If multiple values exist within a 10 min window, the mean of these values is taken as the representative value for that interval. In cases where no values are recorded in a given 10 min period, the value from the preceding interval is carried forward. Employing this methodology, synchronized data with a 10 min time interval is generated, reducing the total dataset size to approximately 138 MB—roughly 1/100th of the original 11 months of raw data, which amounts to 15 GB. Despite this substantial reduction in data volume, the synchronized dataset retains the majority of the plant's operational history.

3.2. Generating Train Data for AI Algorithms

Upon the completion of data synchronization, the next critical step is to generate a training dataset specifically designed for the AI predictive model. The aim of this AI model is to forecast the outlet temperature of natural gas (NG) in the tubes of the heat exchanger after a defined time period. Therefore, the raw data collected from the AAV must be transformed into a format that is suitable for training the predictive model. The training dataset consists of both independent and dependent variables or target variables, the specific details of which are outlined in Table 1. A wide array of values for the independent variables can be collected or extracted from the synchronized data. In the proposed AI model, the outlet temperature after a specific time period—designated as Δt—is the dependent variable. Importantly, observed values of certain variables, such as the vaporization flow rate or the outlet temperature after a Δt time span, may vary even when measurements are taken at the same time point, depending on changes in Δt.

Table 1. Structure of Training Data for AI Algorithms.

Classification	Variable Name	Data Type
Independent Variables	Month	Categorical
	Hour	Categorical
	Day of Week	Categorical
	Cell ID	Categorical
	Consecutive operating time period before the time of measurement (Unit: Minute)	Integer
	Δt (Unit: Minute)	Integer
	Rotational fan speed (Unit: RPM, Constant speed during Δt)	Integer
	The vaporization flow rate during Δt	Float
	Air temperature (Unit: °C)	Float
	Air temperature one hour before the measurement (Unit: °C)	Float
	Air temperature two hours before the measurement (Unit: °C)	Float
	Humidity	Float
	Humidity one hour before the measurement	Float
	Humidity two hours before the measurement	Float
	LNG inlet temperature (Unit: °C)	Float
	Valve angle	Float
	Outlet temperature (Unit: °C)	Float
Dependent Variable	Outlet temperature after a time period of Δt (Unit: °C)	Float

Given the variable nature of Δt, multiple values of the dependent variable may exist at a single measurement time point. Consequently, the size of the training dataset surpasses that of the synchronized data. This procedure essentially serves to augment the data, enabling a more thorough exploration of the initial dataset to extract nuanced insights.

The total size of the training data expands from the 138 MB of the synchronized data to approximately 400 MB. If needed, cell-specific or monthly training datasets are generated and utilized for training the predictive AI model. Additionally, only those independent variables deemed relevant through preliminary analysis are selected for inclusion in the training process.

3.3. Analysis of the Generated Data

A comprehensive data analysis is conducted to elucidate the operational characteristics of the AAV, utilizing both the synchronized data and the training dataset intended for the AI model. In the course of this analysis, the synchronized data serves as the primary source, while in certain instances, supplementary information like power consumption per fan speed is also integrated.

3.3.1. Monthly Fan Speed Analysis

First, an analysis of the monthly fan speeds across all 16 cells over an 11-month operational period was conducted. The results revealed that fan speeds ranged from 400 to 900 RPM. However, 550 RPM was predominantly utilized from May to September, while 600 RPM was the primary choice for the remaining months. Consequently, the available operational data for fan speeds below 500 RPM or above 650 RPM was insufficient for robust AI model training. Such an imbalance in fan speed data could compromise the predictive performance of the AI model.

3.3.2. NG Outlet Temperature Analysis

Second, upon examining the outlet temperatures of natural gas (NG), it was observed that instances of temperatures at or below 5 °C were primarily confined to the winter season. Most of the readings registered temperatures above 5 °C. Notably, when the outlet temperature did fall below this threshold during vaporization operations, it did not gradually decline but rather exhibited a precipitous drop to below 5 °C within a matter of minutes. This abrupt temperature change poses challenges for predictive modeling. Therefore, this characteristic should be carefully integrated into the development of the AI model to enhance its ability to accurately forecast temperature drops below 5 °C after a specified time period (Δt) during vaporization.

3.3.3. Factors Affecting Outlet Temperature

Third, the analysis revealed that even when cells within the same unit operated at identical fan speeds, there could be significant variances in the outlet temperatures among different AAVs at the end of the vaporization process. Additionally, the fluctuation in the NG outlet temperature during vaporization was found to be considerable, which appears to be influenced by the cells' locations. These observations underscore the necessity for a stable vaporization operation strategy aimed at maintaining as consistent an outlet temperature as possible.

3.3.4. Regression Analysis

Lastly, a regression analysis was conducted, employing future discharge temperature as the dependent variable and various other features as independent variables. As indicated in Table 2, the most influential factors on future outlet temperature were found to be the current air temperature, fan speed, and existing NG outlet temperature.

Table 2. Impact Analysis on Future Outlet Temperature (ANOVA Table).

	df	Sum of Square	Mean Square	F-Value
Previously consecutive operating time	1	84,975.4	84,975.4	4388.1
Prediction period	1	17,603.2	17,603.2	909.0
Fan speed	1	297,224.8	297,224.8	15,348.5
Vapo. Flow Rate	1	46,871.2	46,871.2	2420.4
Temp. (Current time)	1	792,558.5	792,558.5	40,927.3
Temp. (One hour before)	1	1657.1	1657.1	85.6
Temp. (Two hours before)	1	199.3	199.3	10.3
Humidity (Current time)	1	4090.9	4090.9	211.3
Humidity (One hour before)	1	1577.0	1577.0	81.4
Humidity (Two hours before)	1	2492.4	2492.4	128.7
LNG inlet temp.	1	7020.7	7020.7	362.5
Current outlet temp.	1	213,413.4	213,413.4	11,020.5
Residual	13,987	270,859.0	19.4	

4. Prediction Model with DNN and Test Results

To predict the temperature of NG at the outlet of the tubes in the heat exchanger after a specific time period (Δt), a deep learning model is designed and applied. Independent variables described in Section 3 are given as input data of the deep neural network (DNN) model and the NG temperature at the outlet of the tubes after a specific time period (Δt) is defined as the output to be predicted. The input/output model structure used in the DNN is shown in Figure 6.

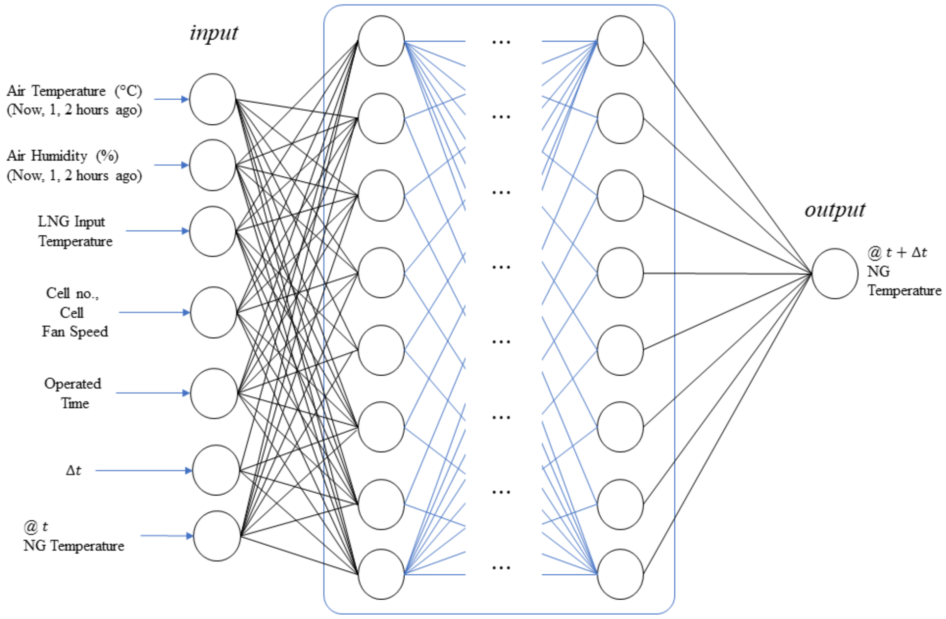

Figure 6. The structure of the DNN model.

We conducted training and testing on various DNN model architectures and selected two models with superior performance, naming them DNN1 and DNN2. The details of the DNN models, such as the number of hidden layers, number of nodes, and activation functions, are summarized in Table 3. The training options set in the Keras software package (version 2.14.0) are listed in Table 4. The raw data of AAV operation is pre-processed and synchronized in 10 min intervals and prepared for use as input/output data. About 70% of the data are used as training data and the remaining 30% are used as test data. Since the fan speed is adjusted every 4 h, the specific time period (Δt) for the next prediction is set to 30 min without loss of generality in the field. The performance indexes used for evaluating the prediction accuracy of the DNN models are Mean Absolute Error (MAE), Mean Square Error (MSE), and R^2 Score.

Table 3. Layer structure of DNN1 and DNN2.

Model	Layer	# of Node	Activation
DNN1	input	11	relu
	hidden 1	256	relu
	hidden 2	256	relu
	hidden 3	256	relu
	hidden 4	256	relu
	output	1	linear
DNN2	input	11	relu
	hidden 1	32	relu
	hidden 2	64	relu
	hidden 3	128	relu
	hidden 4	64	relu
	hidden 5	32	relu
	output	1	linear

Table 4. Keras option set of DNN in training.

Epochs	Batch Size	Loss	Optimizer	Metrics
200	10	MSE	ADAM	MSE, MAE

Figure 7 shows the learning curve of the training loss of a DNN1 model over epochs. As can be observed, the Mean Squared Error (MSE) starts at a high value, indicating a significant discrepancy between the model's predictions and the actual values during the initial stages of training. However, as the training progresses through subsequent epochs, there is a rapid decline in the MSE. This suggests that the model is effectively learning and adjusting its weights to minimize the error. Around the 50th epoch, the decrease in MSE begins to stabilize, indicating that the model has reached a point where further training offers diminishing returns in error reduction.

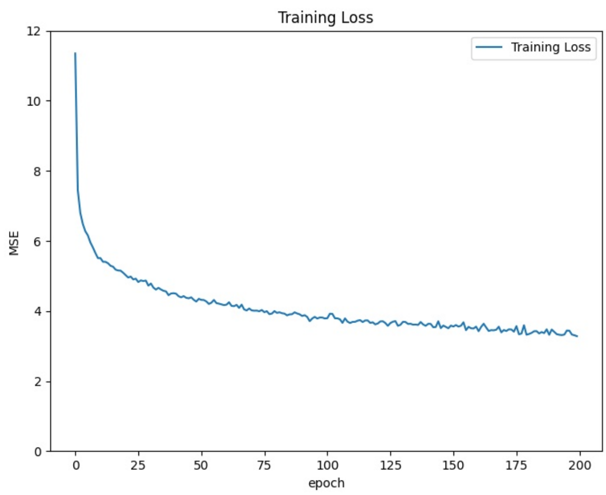

Figure 7. The learning curve of the DNN1 model.

The resulting prediction performance of the proposed DNN models is shown in Table 5. The DNN1 model has an MSE of 3.013 °C and an MAE of 0.935, with an R^2 Score (calculated as 1–SSE/SST, where SSE represents the Sum of Squared Error and SST is the Sum of Squared Total) of 0.961. This indicates the robust performance of the proposed model. The performance of DNN2 is nearly identical to that of DNN1. Despite having different layers, both DNN1 and DNN2 models yielded similar results. From this, it is inferred that the performance of Deep Neural Networks may not be highly sensitive to their architectural variations. Additionally, we trained the following machine learning models and compared their performance to that of the DNN models: Random Forest (RF), Gradient Boosting Regression (GBR), K-Neighbors Regression (K-NR), and Support Vector Regression (SVR). Overall, the performance of RF is comparable to that of DNN1 and DNN2, while the other models did not match the satisfactory results of the DNNs. Notably, while the SVR model exhibited excellent performance on the training data, its performance on the test data was markedly poor, rendering it unsuitable for practical use. This suggests a severe overfitting issue during the training of the SVR model.

Table 5. Prediction performance of DNN and other types of machine learning models.

Model	Train Data Performance			Test Data Performance		
	MSE	MAE	R^2 Score	MSE	MAE	R^2 Score
DNN1	2.662	0.916	0.965	3.013	0.935	0.961
DNN2	3.047	0.953	0.960	3.304	0.970	0.957
Random Forest	4.163	1.098	0.945	4.601	1.123	0.940
Gradient Boosting Regression	14.634	2.911	0.807	14.898	2.929	0.807
K-Neighbors Regression	5.240	1.392	0.931	8.558	1.767	0.889
Supported Vector Regression	0.010	0.100	1.000	77.005	7.474	0.000

In Table 6, the results of prediction are re-grouped into two categories: (1) NG outlet temperature is below 0 °C and (2) overall temperature range of NG outlet. As the prediction accuracy of the NG outlet temperature becomes lower according to Table 6, the prediction error tends to increase for both low-speed RPM and high-speed RPM. It seems that there are unique characteristics in the dataset that result in a prediction inaccuracy for low outlet NG temperatures. Considering the real operation of AAVs in the field, if the outlet temperature of the NG falls below 0 °C, the operator urgently tries to adjust the outlet temperature higher by increasing the fan speed. Therefore, cases of both the outlet temperature of the NG and the fan speed being low are very rare. This imbalanced data characteristic decreases prediction performance at low outlet temperatures and low fan speeds. A more diverse test case should be done in the field and more related data should be collected in order to increase the accuracy across the whole range of temperatures and fan speeds.

Table 6. Variation in prediction performance with RPM and outlet temperature of NG.

Outlet Temperature of NG	Performance Index	Fan Rotation Rate (RPM)			
		400~500	500~600	600~700	700~
Below 0 °C	Training data MAE	1.405	1.541	2.110	1.481
	Training data MSE	5.731	5.843	7.864	6.517
	Training data R^2 Score	0.920	0.919	0.891	0.909
	Test data MAE	25.259	11.202	6.454	10.165
	Test data MSE	777.498	205.662	67.792	210.499
	Test data R^2 Score	−13.803	−7.716	−0.245	−1.094
Overall Temperature Range	Training data MAE	1.452	1.601	1.542	1.470
	Training data MSE	6.136	6.331	6.225	6.405
	Training data R^2 Score	0.915	0.912	0.913	0.911
	Test data MAE	1.031	1.727	1.399	2.486
	Test data MSE	3.636	7.694	4.929	25.345
	Test data R^2 Score	0.641	0.780	0.919	0.736

5. Conclusions

In this study, we embarked on preliminary research with the goal of developing artificial intelligence technology to enhance the efficiency and safety of the entire Ambient Air Vaporizer (AAV) system. Leveraging real operational data collected over approximately one whole year, we gained critical insights. We identified seasonality in both production and energy costs and through regression and variance analyses, found that future natural gas (NG) outlet temperatures are significantly influenced by current atmospheric conditions, fan speeds, and existing NG outlet temperatures.

Building on these findings, a Deep Neural Network (DNN) prediction model was subsequently developed. This model is capable of predicting the outlet temperature of vaporized NG after a given time interval. Given the operational constraints—namely, a limited range of fan speeds and safety-oriented guidelines—the task of developing an effective prediction model presented unique challenges. To overcome these, we evaluated various learning models under diverse conditions, ultimately arriving at a DNN model with minimized absolute mean error (MAE) and mean square error (MSE).

With its multiple potential applications, the artificial intelligence model serves as a valuable tool, primarily for facility operators. It can provide customized, efficient AAV operational policies based on specific environmental conditions and LNG inlet flow rates. Looking ahead, we aim to expand this work by integrating the proposed DNN prediction model into a production simulation framework. This integration will pave the way for the development of optimal production strategies, leading to more intelligent facility operations.

Author Contributions: Methodology, J.-H.S. and J.-Y.B.; Software, J.-Y.B.; Validation, G.-C.L.; Formal analysis, S.-K.L. and J.-G.K.; Investigation, S.-K.L.; Resources, J.-G.K.; Data curation, G.-C.L.; Writing—original draft, J.-H.S. and J.-Y.B. All authors have read and agreed to the published version of the manuscript.

Funding: This research was funded by Ministry of Science and ICT grant number IITP-2023-RS-2023-00260175.

Data Availability Statement: Data available on request due to restrictions. The data presented in this study are available on request from the corresponding author, provided that permission is granted by Korean Gas Corporation. The data are not publicly available due to protection of intellectual property of Korean Gas Corporation.

Acknowledgments: This research was supported by the MSIT (Ministry of Science and ICT), Korea, under the ICAN (ICT Challenge and Advanced Network of HRD) support program (IITP-2023-RS-2023-00260175) supervised by the IITP (Institute for Information & Communications Technology Planning & Evaluation).

Conflicts of Interest: The authors declare no conflict of interest. The funders had no role in the design of the study; in the collection, analyses, or interpretation of data; in the writing of the manuscript; or in the decision to publish the results.

References

1. Zhang, Y.; Ren, S.; Liu, Y.; Si, S. A big data analytics architecture for cleaner manufacturing and maintenance processes of complex products. *J. Clean. Prod.* **2017**, *142*, 626–641. [CrossRef]
2. Reddy, H.V.; Bisen, V.S.; Rao, H.N.; Dutta, A.; Garud, S.S.; Karimi, I.A.; Farooq, S. Towards energy-efficient LNG terminals: Modeling and simulation of reciprocating compressors. *Comput. Chem. Eng.* **2019**, *128*, 312–321. [CrossRef]
3. Walther, J.; Spanier, D.; Panten, N.; Abele, E. Very short-term load forecasting on factory level–A machine learning approach. *Procedia CIRP* **2019**, *80*, 705–710. [CrossRef]
4. Park, C.Y.; Kim, J.W.; Kim, B.; Lee, J. Prediction for manufacturing factors in a steel plate rolling smart factory using data clustering-based machine learning. *IEEE Access* **2020**, *8*, 60890–60905. [CrossRef]
5. Mohamadi, S.; Ehteram, M.; El-Shafie, A. Accuracy enhancement for monthly evaporation predicting model utilizing evolutionary machine learning methods. *Int. J. Environ. Sci. Technol.* **2020**, *17*, 3373–3396, Erratum in *Int. J. Environ. Sci. Technol.* **2022**, *19*, 4611–4612. [CrossRef]

6. Carvalho, T.P.; Soares, F.A.; Vita, R.; Francisco, R.D.P.; Basto, J.P.; Alcalá, S.G. A systematic literature review of machine learning methods applied to predictive maintenance. *Comput. Ind. Eng.* **2019**, *137*, 106024. [CrossRef]
7. Westphal, E.; Seitz, H. A machine learning method for defect detection and visualization in selective laser sintering based on convolutional neural networks. *Addit. Manuf.* **2021**, *41*, 101965. [CrossRef]
8. Zhang, T.; Ding, B.; Zhao, X.; Liu, G.; Pang, Z. LearningADD: Machine learning based acoustic defect detection in factory automation. *J. Manuf. Syst.* **2021**, *60*, 48–58. [CrossRef]
9. Adib, H.; Sabet, A.; Naderifar, A.; Adib, M.; Ebrahimzadeh, M. Evolving a prediction model based on machine learning approach for hydrogen sulfide removal from sour condensate of south pars natural gas processing plant. *J. Nat. Gas Sci. Eng.* **2015**, *27*, 74–81. [CrossRef]
10. Zhou, L.; Garg, D.; Qiu, Y.; Kim, S.M.; Mudawar, I.; Kharangate, C.R. Machine learning algorithms to predict flow condensation heat transfer coefficient in mini/micro-channel utilizing universal data. *Int. J. Heat Mass Transf.* **2020**, *162*, 120351. [CrossRef]
11. Wood, D.A. Predicting saturated vapor pressure of LNG from density and temperature data with a view to improving tank pressure management. *Petroleum* **2021**, *7*, 91–101. [CrossRef]
12. Jeong, H.M.; Chung, H.S.; Lee, S.C.; Kong, T.W.; Yi, C.S. Optimum design of vaporizer fin with liquefied natural gas by numerical analysis. *J. Mech. Sci. Technol.* **2006**, *20*, 545–553. [CrossRef]
13. Kim, N.K.; Yun, S.K. Study on the LNG vaporization characteristics of Open Rack Vaporizer (ORV) with two-way seawater supplying system. *J. Korean Inst. Gas* **2019**, *23*, 41–46.
14. Le Gall, R. *Experimental Study and Modeling of Frost Formation in Heat Exchangers (Etude Experimentale et Modelisation du Phenomene de Givrage dans les Echangeurs de Chaleur)*; National Polytechnic Institute: Grenoble, France, 1994.
15. Lee, Y.; Na, J.; Lee, W.B. Robust design of ambient-air vaporizer based on time-series clustering. *Comput. Chem. Eng.* **2018**, *118*, 236–247. [CrossRef]
16. Ma, G.; Zhang, C.; Zhao, L. Analysis on heat transfer effect of air-temperature vaporizer in LNG satellite station. *Adv. Mech. Eng.* **2017**, *9*, 1687814017711856. [CrossRef]
17. Shin, Y.; Yoo, S.; Kwak, D.; Lee, N.; Shin, D. AutoML and Artificial Neural Network Modeling of Process Dynamics of LNG Regasification Using Seawater. *Korean Chem. Eng. Res.* **2021**, *59*, 209–218.
18. Chen, C.; Wei, J.; Li, Z. Remaining useful life prediction for lithium-ion batteries based on a hybrid deep learning model. *Processes* **2023**, *11*, 2333. [CrossRef]